

Communication

## Ruthenium-vinylhelicenes: remote metal-based enhancement and redox switching of the chiroptical properties of a helicene core.

Emmanuel Anger, Monika Srebro, Nicolas Vanthuyne, Loic Toupet, Stephane Rigaut, Christian Roussel, Jochen Autschbach, Jeanne Crassous, and Regis Reau

*J. Am. Chem. Soc.*, **Just Accepted Manuscript** • DOI: 10.1021/ja304424t • Publication Date (Web): 20 Jun 2012

Downloaded from <http://pubs.acs.org> on June 24, 2012

### Just Accepted

“Just Accepted” manuscripts have been peer-reviewed and accepted for publication. They are posted online prior to technical editing, formatting for publication and author proofing. The American Chemical Society provides “Just Accepted” as a free service to the research community to expedite the dissemination of scientific material as soon as possible after acceptance. “Just Accepted” manuscripts appear in full in PDF format accompanied by an HTML abstract. “Just Accepted” manuscripts have been fully peer reviewed, but should not be considered the official version of record. They are accessible to all readers and citable by the Digital Object Identifier (DOI®). “Just Accepted” is an optional service offered to authors. Therefore, the “Just Accepted” Web site may not include all articles that will be published in the journal. After a manuscript is technically edited and formatted, it will be removed from the “Just Accepted” Web site and published as an ASAP article. Note that technical editing may introduce minor changes to the manuscript text and/or graphics which could affect content, and all legal disclaimers and ethical guidelines that apply to the journal pertain. ACS cannot be held responsible for errors or consequences arising from the use of information contained in these “Just Accepted” manuscripts.

# Ruthenium-vinylhelicenes: remote metal-based enhancement and redox switching of the chiroptical properties of a helicene core.

Emmanuel Anger,<sup>†</sup> Monika Srebro,<sup>‡,£</sup> Nicolas Vanthuyne,<sup>§</sup> Loïc Toupet,<sup>†</sup> Stéphane Rigaut,<sup>†</sup> Christian Roussel,<sup>§</sup> Jochen Autschbach,<sup>\*,‡</sup> Jeanne Crassous,<sup>\*,†</sup> and Régis Réau<sup>\*,†</sup>

<sup>†</sup> Institut des Sciences Chimiques de Rennes, UMR 6226, Institut de Physique de Rennes, UMR 6251, Campus de Beaulieu, CNRS-Université de Rennes 1, 35042 Rennes Cedex, France. <sup>‡</sup> Department of Chemistry, University at Buffalo, State University of New York, Buffalo, NY 14260, USA. <sup>£</sup> Faculty of Chemistry, Jagiellonian University, 30-060 Krakow, Poland. <sup>§</sup> Chirosciences, UMR 7313, Stéréochimie Dynamique et Chiralité, Aix-Marseille University, 13397 Marseille Cedex 20, France

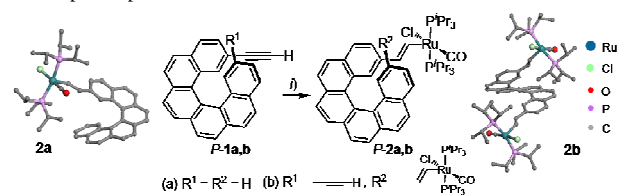
Supporting Information Placeholder

**ABSTRACT:** Introducing metal-vinyl ruthenium moieties onto [6]helicene results in a significant enhancement of the chiroptical properties due to strong metal-ligand electronic interactions. The electro-active Ru-centers allow the achievement of the first purely helicene-based redox-triggered chiroptical switches. A combination of electrochemical, spectroscopic and theoretical techniques reveals that the helicene moiety is a non-innocent ligand bearing a significant spin density.

The molecular engineering of [n]helicene derivatives is a subject of intensive research due to their large-magnitude chiroptical properties which are of great interest for manifold applications in chiral material sciences such as nonlinear optics, waveguides, switches, luminescent materials or sensors.<sup>1</sup> The main challenge for the development of [n]helicenes towards functional materials is the discovery of efficient synthetic routes and simple strategies to improve and tune their chiroptical properties. In this regard, the most efficient general strategy developed up to now involves the modification of their ‘screw-shaped’ *ortho*-fused polycyclic  $\pi$ -framework, since the unique chiroptical properties of helicenes are inherently linked to this helicoidal conjugated skeleton. This approach includes for example the modification of the helical pitch, the increase of the number of fused aromatic rings, or the incorporation of heteroatoms or transition metals within the  $\pi$ -skeleton.<sup>1,2</sup>

Herein, we describe an original strategy for the molecular engineering of helicenes based on introducing *lateral organometallic substituents* on a ‘screw-shaped’ *ortho*-fused polycyclic  $\pi$ -framework. The versatility of this original approach is illustrated with the synthesis of mono- and bis(vinyl-Ru<sup>II</sup>)[6]helicenes **2a,b** (Scheme 1). The d<sup>6</sup> ruthenium ion was selected since (i) it displays very efficient electronic coupling with unsaturated organic ligands,<sup>3a,b,4</sup> and (ii) its organometallic complexes are electro-active at fairly low potentials, allowing the synthesis of redox-triggered NLO-active<sup>3c</sup> and optical<sup>3d,f</sup> switches. Remarkably, introducing these remote Ru<sup>II</sup>-centers results in a significant change of the chiroptical properties of helical  $\pi$ -cores **1a,b**. Furthermore, the redox properties of the lateral Ru<sup>II</sup> metal centers allow the corresponding radical cations to be easily

generated. This redox process significantly impacts the chiroptical properties of the helicene core, affording the first purely helicene-based redox chiroptical switch.<sup>5</sup> These results on closed- and open-shell complexes are rationalized with the help of first-principles calculations.



**Scheme 1.** Synthesis and X-ray crystallographic structures (H atoms have been omitted) of enantiopure *P*-complexes **2a,b**.  $\eta$  HRu(CO)Cl(PPr<sub>3</sub>)<sub>2</sub>, CH<sub>2</sub>Cl<sub>2</sub>, r.t., Ar.

Mono- and bis-(ethynyl)carbo[6]helicenes **1a** and **1b**<sup>6</sup> (Scheme 1) were obtained using classic photocyclization reactions<sup>1a,e</sup> and resolved (*ee* > 99%) by chiral HPLC separation (SI). Following the well-established stereoselective hydorruthenation of alkynes,<sup>4</sup> **1a,b** were reacted with HRu(CO)Cl(PPr<sub>3</sub>)<sub>2</sub> affording the organometallic derivative **2a,b** (Scheme 1) as air stable dark red solids (yields: **2a**, 90%; **2b**, 80%). Their NMR data fully support the proposed structures, especially the presence of *trans*-vinyl ruthenium-substituted moieties and two non-equivalent PPr<sub>3</sub> ligands due to the presence of the helicene cores (SI). The X-ray diffraction study of Ru<sup>II</sup>-capped helicenes **2a,b** (Scheme 1, SI), shows that the helical angles (dihedral angles between the terminal rings of the helix) are slightly different for these two complexes (**2a**, 49.7°; **2b**, 60.9°), but in the usual range ob-

served for [6]helicene derivatives.<sup>2j</sup> The geometry around the five-coordinated Ru<sup>II</sup>-centers is square pyramidal, with the two *trans* PPr<sub>3</sub>, the Cl and the CO ligands forming the basis of the pyramid and the vinyl-helicene moiety being at the apical position. The Ru-C1-C2-C3 bond lengths (**2a**: 1.980, 1.337 and 1.464 Å) are typical for *trans* vinyl-Ru complexes,<sup>4c</sup> and the vinyl-Ru moiety is almost coplanar with the helicene part (Ru-C1-C2-C3: **2a**, 176.33°; **2b**, 168.98°), allowing efficient metal-ligand electronic interaction through the carbon-carbon double bonds. This feature was confirmed by UV-vis spectroscopy of complexes **2a,b** which displayed large low-energy bands between 380 nm and 460 nm (SI) that do not exist in their organic precursors **1a,b**. BHLYP/SV(P) TDDFT calculations following geometry optimizations with BP/SV(P) (SI), clearly confirm the presence of this electronic interaction. For example, the HOMO(206) of **2a** spans over the metal and the vinyl-helicene moiety (Figure 1, top).

The comparison of the chiroptical properties<sup>7</sup> of derivatives **1a,b** and their Ru<sup>II</sup>-modified derivatives **2a,b** revealed a remarkable and unexpected feature. Upon introducing the remote metal centers, the molar rotations (MRs) values are doubled ( $[\phi]_D^{25}$  in °cm<sup>2</sup>/dmol: **1a/2a**, ±11030/23770; **1b/2b**, ±20000/39150)! The difference in the chiroptical properties of **1a,b** and **2a,b** is also reflected in their corresponding electronic circular dichroism (ECD) spectra. Note that the shape of the CD spectra of organic helicenes **1a** and **1b** are similar, with higher band intensity for **1b** (Figure 2). The experimental ECD of **P-1a** and **P-2a** show two intense ECD bands at 250 nm (negative) and 335 nm (positive) which are the fingerprint of helicene derivatives (Figure 2a). Indeed, according to the calculations, the excitation n<sup>o</sup>6 (325 nm) with the strongest calculated rotatory strength of **2a** corresponds well to the excitation n<sup>o</sup>3 (312 nm, Figure 1 top) of the organic derivative **1a** in the sense that similar MOs centered on the π-conjugated helical platform are involved (Table S7). The comparison of the experimental ECD spectra of **P-1a** and **P-2a** also shows new low energy bands of moderate magnitude for **2a** (380 nm – 460 nm, Figure 1 top) that involve metal contribution. For example, **P-2a** excitations n<sup>o</sup>5 and n<sup>o</sup>3 correspond mainly (58% and 65%) to ππ\* transitions localized in the helicene moiety with visible metal orbital involvement (HOMO(206)-LUMO+1(208) and HOMO(206)-LUMO(207), Figure 1). Furthermore, excitation n<sup>o</sup>2 involves dominantly MOs centered on the metal fragment (MO(200): formally a t<sub>2g</sub> orbital with carbonyl π\*-backbonding character; MO(209): a metal-centered orbital, Figure 1). It is possible that this particular excitation is somewhat too red-shifted in the calculations,<sup>7b</sup> but the overall spectral envelopes agree well with experiment. These additional ECD bands at long wavelengths having large contribution from the metal atom are responsible for the increase of the molar rotation observed in **2a**. The most intense CD-active bands of **2b** displaying the highest Δε values were found between 380 and 430 nm and a separate band at low energy (450 nm) is now clearly observable.

This red shift of the ECD spectrum upon introducing the two Ru<sup>II</sup>-centres is well-reproduced by theory (Figure 1 bottom, SI). The **P-2b** excitation with the strongest rotatory strength (n<sup>o</sup>12, calculated at 315 nm) affords two main contribution

from HOMO-2(324)-to-LUMO(327) and HOMO-2(324)-to-LUMO+1(328), respectively (Table S7, Figure 1 bottom).

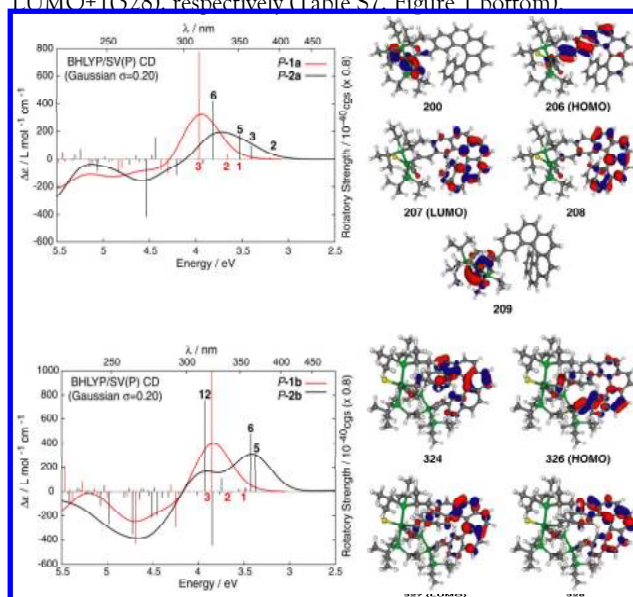


Figure 1. Calculated (BHLYP/SV(P)) CD spectra of **P-1a** (red line) vs. **P-2a** (black) (top) and **P-1b** (red) vs. **P-2b** (black) (bottom), and isosurfaces (0.04 au) of selected MOs of **2a** (top) and **2b** (bottom) involved in the transitions. Compare SI.

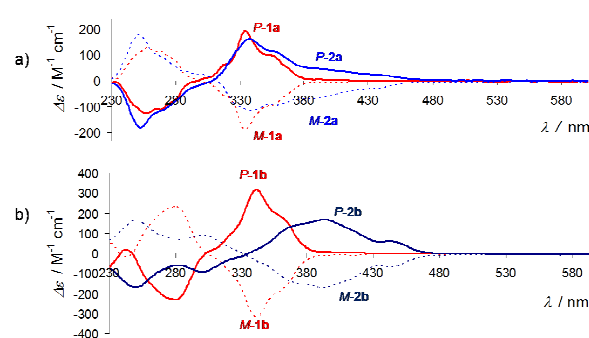


Figure 2. CD spectra in CH<sub>2</sub>Cl<sub>2</sub> at 293 K of a) mono-alkynyl precursors **P**(+)- and **M**(-)-**1a** and their corresponding mono-vinylruthenium **P**(+)- and **M**(-)-**2a**, and b) of bis-alkynyl precursors **P**(+)- and **M**(-)-**1b** and their corresponding bis-vinylruthenium **P**(+)- and **M**(-)-**2b**.

Both contributions involve orbitals predominantly centered within the helical π-system, with negligible metal character. Two other intense excitations (n<sup>o</sup>5 and n<sup>o</sup>6) are located at ~365 nm and constitute the new positive band of the CD spectra. Their dominant contributions correspond to, respectively, HOMO(326)-to-LUMO(327) and HOMO(326)-to-LUMO+1(328) products and display a partial charge-transfer character of ππ\* excitations within the helicene ligand enhanced by the involvement of *d* orbitals of both metal centers. Such excitations (n<sup>o</sup>6 and n<sup>o</sup>5) in **2b** were also found in the case of **2a** (n<sup>o</sup>5 and n<sup>o</sup>3) although with a substantially lower intensity. Therefore, their increased intensity can account for the intensity enhancement of the low-energy tail of the positive CD band in the **P-2b** and consequently for the MR enhancement.

These results illustrate the power and simplicity of organometallic chemistry to produce new chiral molecular architectures and to increase of the chiroptical properties of the helicene platforms.

The remote Ru<sup>II</sup>-metal centres also endow the helicene core with unprecedented chiroptical redox-triggered switching property, due to their electro-active behaviour. Chiroptical switches are multifunctional materials that may be useful for a variety of application such as molecular electronics, optical displays or telecommunication purposes.<sup>5,8</sup> It is noteworthy that redox triggered chiral switches are still quite rare<sup>5a</sup> and that very few helicene-based chiroptical switches have been described so far, almost all being based on photochromic systems.<sup>9</sup> In addition, although examples of electro-active helicene derivatives have been described in the literature,<sup>5b,10</sup> only one was considered as a potential redox chiral switch.<sup>5b</sup> Therefore, the electrochemical behaviour of organometallic species **2a,b** was investigated with the aim to obtain the first purely helicene-based redox chiral switches. An important and well-established property of (arylvinylyl)RuCl(CO)(P<sup>i</sup>Pr<sub>3</sub>)<sub>2</sub> complexes is their multistep reversible oxidation/reduction processes at fairly low potentials, involving the 'non-innocent' arylvinyl ligands. In fact, the RuCl(CO)(P<sup>i</sup>Pr<sub>3</sub>)<sub>2</sub> moiety stabilizes the radical cations to about the same extent as dialkylamino groups, and the charges are mainly located on the organic arylvinyl fragments.<sup>4c</sup> Cyclic voltammetry (CV) studies of **2a** (CH<sub>2</sub>Cl<sub>2</sub>/NBu<sub>4</sub>PF<sub>6</sub>, 0.2 M) revealed the presence of one chemically and electrochemically reversible oxidation at  $E_1^\circ = +0.173$  V vs. the ferrocene/ferrocenium (Fc/Fc<sup>+</sup>) standard, followed by a second irreversible oxidation at  $E_{pa} = +0.781$  V (100 mV s<sup>-1</sup>) (SI). A full reversibility of the process was observed upon several oxidation/reduction cycles between 0 V and 0.4 V (SI). Interestingly, the one-electron oxidation at  $E_1^\circ = +0.173$  V affording [2a]<sup>•+</sup>PF<sub>6</sub><sup>-</sup>,<sup>4c</sup> takes place at a significantly lower potential than that observed for thiophene-based helicenes (+1.3 V),<sup>10d</sup> rendering the helicene core easy to oxidize. The bis(Ru<sup>II</sup>)-[6]-helicene **2b** (Scheme 1) was also investigated since it bears two redox active moieties and is therefore a unique platform to investigate the impact of multi-oxidation processes on the electronic property of the prototype [6]-helicene fragment. Two consecutive reversible one-electron oxidation waves were observed at  $E_1^\circ = +0.146$  and  $E_2^\circ = +0.285$  V (vs. Fc/Fc<sup>+</sup>) accompanied by a third chemically irreversible wave at ca.  $E_{pa} = +0.83$  V (v 100 mV s<sup>-1</sup>) (SI). The splitting of the first two waves (~130 mV) suggests a stepwise oxidation of the redox-active bis(Ru<sup>II</sup>)-[6]-helicene **2b** to [2b]<sup>•+</sup> and [2b]<sup>2+</sup>, with substantial comproportionation ( $K_c \sim 234$ , i.e. ~90% of the monoradical cation upon full one electron oxidation).<sup>3e</sup>

These redox processes were monitored by UV/vis/NIR spectroelectrochemical spectroscopy in a transparent thin-layer (OTTLE) cell in dichloroethane (DCE) solutions (see SI). The formation of the radical cation [2a]<sup>•+</sup> results in a slight decrease of high energy bands (< 480 nm), the appearance of sets of structured absorptions at ~500 nm, and two lower-energy absorption bands at ~630 and ~1000 nm (see SI). The formation of [2b]<sup>•+</sup> and [2b]<sup>2+</sup> was also monitored and showed three sets of new bands appearing during the first oxidation stage, the first one between 450-600 nm, a second one at 650 nm, and a large extended band centered at 950 nm (see SI). Upon further ox-

idation from 0.2 to 0.6 V (vs. Fc/Fc<sup>+</sup>), all these bands (450-600 and 950 nm) disappeared and a new one appeared at 700 nm (SI).

In the spectroelectrochemical IR spectrum of **2a**, a blue shift of the CO stretch from 1913 to 1968 cm<sup>-1</sup> (Figure 3) and the appearance of new C=C bands in the 1640-1520 cm<sup>-1</sup> region (SI) with clean isobestic points were also observed during the formation of [2a]<sup>•+</sup>. This slight increase of the energy of the CO stretch is assigned to a decrease of electron density transferred from the metal atom to the π\* orbitals of the carbonyl ligand that is weaker than for a purely metal based oxidation.<sup>4</sup> Thus, this fact suggests that the radical cation is largely localized on the helicene fragment.<sup>4c</sup> Similarly, the mono-oxidation of **2b**, displaying one CO stretch at 1911 cm<sup>-1</sup>, results in two CO stretches at 1913 and 1965 cm<sup>-1</sup> of identical intensities (see SI) that are testimonies of two non equivalent ruthenium centers on the IR timescale in [2b]<sup>•+</sup>.<sup>4c,d</sup>

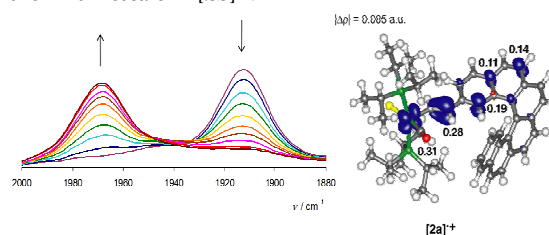


**Figure 3.** IR region of the  $\nu(\text{CO})$  stretch upon mono-oxidation of **2a**. B3LYP/SV(P) electron spin density,  $\Delta\rho = \rho^\alpha - \rho^\beta$ , in [2a]<sup>•+</sup>. Numbers listed are fractions of the total integrated spin density obtained from Mulliken decompositions of  $\Delta\rho$ .

Upon the second oxidation, these two bands disappear and a new  $\nu(\text{CO})$  at 1968 cm<sup>-1</sup> grows up. The 'non-innocent' character of the vinylhelicene ligand in [2a]<sup>•+</sup> and [2b]<sup>•+</sup> was confirmed by EPR measurements, with average g values close to  $g_e$  (see SI). Finally, theoretical analyses (B3LYP/SV(P)) of the electronic structure of the radical cations [2a]<sup>•+</sup>, [2b]<sup>•+</sup> and [2b]<sup>2+</sup> (in its singlet and triplet state) were performed. The plots of the electron spin density clearly show that the unpaired charge density is not only localized on the metal atoms but also spread out over the helicene π-ligand (Figure 3 for [2a]<sup>•+</sup> and SI). Thus, in the case of [2b]<sup>•+</sup>, these data cannot be straightforwardly analysed according to the concept of mixed-valence and Robin and Day classification.<sup>3a,b,4c,d</sup> Note that i) the electron spin density and the Singly Occupied Molecular Orbitals (SOMOs) exhibit a general picture revealing a similar spatial distribution of the electron-hole pair, and ii) the SOMOs of [2a]<sup>•+</sup>/[2b]<sup>•+</sup> display the same characteristics as the HOMOs of the neutral systems **2a/2b**, indicating that oxidation results in little reorganization of the organometallic helicene (SI).

The fact that the helicene moiety bears a significant spin density in the oxidized organometallic species, due to the peculiar property of the Ru(CO)Cl(P<sup>i</sup>Pr<sub>3</sub>)<sub>2</sub> fragment, leads to the expectation that the reversible redox processes could impact the chiroptical behaviour. Indeed, the ECD spectra of **P-2a** and **P-[2a]<sup>•+</sup>PF<sub>6</sub><sup>-</sup>** in DCE have noteworthy different features (Figure 4a). The oxidation of **P-2a** results in a significant decrease of the ECD-active bands at 340 nm ( $\Delta(\Delta\epsilon) = -45$  M<sup>-1</sup> cm<sup>-1</sup>), and the

appearance of new broad ECD-active bands (of positive sign for the *P*-stereoisomer) ranging from 430 nm to 580 nm ( $\Delta(\Delta\epsilon) = +17 \text{ M}^{-1} \text{ cm}^{-1}$  at 500 nm) and in the NIR-region ( $\Delta(\Delta\epsilon) = +8.7 \text{ M}^{-1} \text{ cm}^{-1}$  at 900 nm, Figure 4b). Exploiting these differences, along with the reversibility of the redox processes, the first electrochemical chiral switch based on a pure helicene moiety was achieved. More specifically, stepping potentials between  $-0.4$  and  $+0.4 \text{ V}$  of a DCE solution of **2a** ( $0.2 \text{ M}$ ,  $n\text{-Bu}_4\text{PF}_6$ ) in an electrochemical cell leads to a fully reversible modulation of the CD signals both at 340 and 500 nm (Figure 4c) over several cycles. Remarkably, this redox chiroptical switch can be used both at a high-energy wavelength, which belongs to the classic CD-active fingerprint of helicene derivatives, and at a low-energy wavelength, which is due to the presence of the Ru-center (*vide supra*). Likewise, the bis(vinylRu)-system *P*-**2b**/*P*-**[2b]<sup>•+</sup>** also behaves as a reversible electrochemical chiroptical switch at 500 nm ( $\Delta(\Delta\epsilon) = +20 \text{ M}^{-1} \text{ cm}^{-1}$ ) upon stepping potentials between remarkably low working potentials ( $-0.2/+0.2 \text{ V}$ ) (see SI). These results clearly show the significant influence of the Ru(CO)Cl( $\text{P}^i\text{Pr}_3$ )<sub>2</sub> fragment on the electronic and chiroptical properties of the helicene core.

In conclusion, grafting a Ru<sup>II</sup>-ion on a conjugated lateral substituent allows an engineering of helicene chiroptical properties to be performed without modifying the *ortho*-fused  $\pi$ -system. This hitherto unprecedented molecular engineering of helicene derivatives based on organometallic chemistry, which is extremely simple from a synthetic point of view, opens new perspectives in the design of new advanced chiral multifunctional materials.

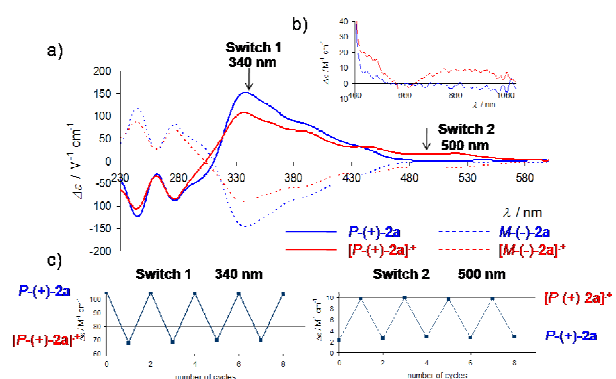


**Figure 4.** a) CD spectra of *P*(+) / *M*(-) enantiomers of **2a** and of their oxidized species in DCE at room temperature. b) NIR-CD region spectra of *P*(-)-**2a** (blue) and *P*(-)-**[2a]<sup>•+</sup>** (red). c) Redox chiroptical switching *P*(+)-**2a**  $\leftrightarrow$  **[P(+)-2a]<sup>•+</sup>** observed by CD spectroscopy at 340 and 500 nm.

## ASSOCIATED CONTENT

**Supporting Information.** Experimental details, CIF files, electrochemical and spectroscopic data of the products. Computational details for theoretical calculations, additional calculated data. This material is available free of charge via the Internet at <http://pubs.acs.org>.

## AUTHOR INFORMATION

**Corresponding Author.** \* [jeanne.crassous@univ-rennes1.fr](mailto:jeanne.crassous@univ-rennes1.fr), [regis.reau@univ-rennes1.fr](mailto:regis.reau@univ-rennes1.fr), [jochena@buffalo.edu](mailto:jochena@buffalo.edu)

## ACKNOWLEDGMENT

We thank the Ministère de l'Éducation Nationale, de la Recherche et de la Technologie, and the Centre National de la Recherche Scientifique (CNRS). L. Norel, Y.-M. Hervault, G. Grelot and O. Cadour are warmly thanked for their kind help in spectroelectrochemical and EPR measurements. The theoretical component of this work has received financial support by the National Science Foundation (CHE 0952253). MS and JA acknowledge the Center for Computational Research (CCR) at the University at Buffalo for providing computational resources. MS is grateful for financial support from the Foundation for Polish Science ('START' scholarship) as well as from Polish Ministry of Science and Higher Education ('Mobility Plus' program).

## REFERENCES

- (a) Martin, R. H. *Angew. Chem. Int. Ed.* **1974**, *13*, 649-659. (b) Katz, T. J. *Angew. Chem. Int. Ed.* **2000**, *39*, 1921-1923. (c) Urbano, A. *Angew. Chem. Int. Ed.* **2003**, *42*, 3986-3989. (d) Rajca, A.; Miyasaka, M. in *Functional Organic Materials* (Eds.: Müller, T. J. J.; Bunz, U. H. F.), Wiley-VCH, Weinheim, **2007**, pp. 543-577. (e) Shen, Y.; Chen, C.-F. *Chem. Rev.* **2012**, *112*, 1463-1535.
- Selected examples: (a) Zak, J. K.; Miyasaka, M.; Rajca, S.; Lapkowski, M.; Rajca, A. *J. Am. Chem. Soc.* **2010**, *132*, 3246-3247. (b) Sehnal, P. et al. *PNAS* **2009**, *106*, 13169-13174. (c) Chen, J.-D.; Lu, H.-Y.; Chen, C.-F. *Chem. Eur. J.* **2010**, *16*, 11843-11846. (d) Pieters, G.; Gaucher, A.; Prim, D.; Marrot, J. *Chem. Comm.* **2009**, *32*, 4827-4828. (e) Harrowen, D. C.; Guy, I. L.; Nanson, L. *Angew. Chem. Int. Ed.* **2006**, *45*, 2242-2245. (f) Guin, J.; Besnard, C.; Lacour, J. *Org. Lett.* **2010**, *12*, 1748-1751. (g) Rasmusson, T.; Martyn, L. J. P.; Chen, G.; Lough, A.; Oh, M.; Yudin, A. K. *Angew. Chem. Int. Ed.* **2008**, *47*, 7009-7012. (h) Sawada, Y.; Furumi, S.; Takai, A.; Takeuchi, M.; Noguchi, K.; Tanaka, K. *J. Am. Chem. Soc.* **2012**, *134*, 4080-4083. (i) Norel, L.; Rudolph, M.; Vanthuyne, N.; Williams, J. A. G.; Lescop, C.; Roussel, C.; Autschbach, J.; Crassous, J.; Réau, R. *Angew. Chem. Int. Ed.* **2010**, *49*, 99-102. (j) Anger, E.; Rudolph, M.; Norel, L.; Zrig, S.; Shen, C.; Vanthuyne, N.; Toupet, L.; Williams, J. A. G.; Roussel, C.; Autschbach, J.; Crassous, J.; Réau, R. *Chem. Eur. J.* **2011**, *17*, 14178-14198.
- (a) Costuas, K.; Rigaut, S. *Dalton Transactions* **2011**, *40*, 5643-5658. (b) Aguirre-Etcheverry, P.; O'Hare, D. *Chem. Rev.* **2010**, *110*, 4839-4864. (c) Samoc M.; Gauthier, N.; Cifuentes, M. P.; Paul, F.; Lapinte, C.; Humphrey, M. G. *Angew. Chem. Int. Ed.* **2006**, *45*, 7376-7379. (d) Di Piazza, E.; Norel, L.; Costuas, K.; Bourdolle, A.; Maury, O.; Rigaut S. *J. Am. Chem. Soc.* **2011**, *133*, 6174-6176. (e) Liu, Y.; Lagrost, C.; Costuas, K.; Tchouar, N.; Le Bozec H.; Rigaut S. *Chem. Commun.* **2008**, 6117-6119. (f) Tanaka, Y.; Ishisaka, T.; Inagaki, A.; Koike, T.; Lapinte, C.; Akita M. *Chem. Eur. J.* **2010**, *16*, 4762-4776. (g) Connelly, N. G.; Geiger, W. E. *Chem. Rev.* **1996**, *96*, 877-910.
- (a) Werner, H.; Esteruelas, M.; Orto, H. *Organometallics* **1986**, *5*, 2295-2299. (b) Zalis, S.; Winter, R. F.; Kaim, W. *Coord. Chem. Rev.* **2010**, *254*, 1383-1396. (c) Maurer, J.; Linseise, M.; Sarkar, B.; Schwederski, B.; Niemeyer, M.; Kaim, W.; Zalis, S.; Anson, C.; Zabel, M.; Winter, R. F. *J. Am. Chem. Soc.* **2008**, *130*, 259-268. (d) Maurer, J.; Sarkar, B.; Schwederski, B.; Kaim, W.; Winter, R. F.; Zalis S. *Organometallics* **2006**, *25*, 3701-3712. (e) Pevny, F.; Di Piazza, E.; Norel, L.; Drescher, M.; Winter, R. F.; Rigaut, S. *Organometallics* **2010**, *29*, 5912-5918.
- (a) Canary, J. W. *Chem. Soc. Rev.* **2009**, *38*, 747-756. (b) Nishida, J.; Suzuki, T.; Ohkita, M.; Tsuji, T. *Angew. Chem. Int. Ed.* **2001**, *40*, 3251-3254.
- Fox, J. M.; Lin, D.; Itagaki, Y.; Fujita, T. *J. Org. Chem.* **1998**, *63*, 2031-2038.
- (a) Furche, F.; Ahlrichs, R.; Wachsmann, C.; Weber, E.; Sobanski, A.; Vogtle, F.; Grimme, S. *J. Am. Chem. Soc.* **2000**, *122*, 1717-1724. (b) Rudolph, M.; Ziegler, T.; Autschbach, J. *Chem. Phys.* **2011**, *391*, 92-100. (c) Newman, M. S.; Lednicer, D. *J. Am. Chem. Soc.* **1956**, *78*, 4765-4770.
- (a) *Molecular Switches*, B. L. Feringa, W.R. Browne (Eds), Wiley-VCH, **2001**. (b) Li, D.; Wang, Z. Y.; Ma, D. *Chem. Commun.* **2009**, 1529-1531.
- (a) Wigglesworth, T. J.; Sud, D.; Norsten, T. B.; Lekhi, V. S.; Branda, N. R. *J. Am. Chem. Soc.* **2005**, *127*, 7272-7273. (b) Wang, Z. Y.; Todd, E. K.; Meng, X. S.; Gao, J. P. *J. Am. Chem. Soc.* **2005**, *127*, 11552-11553.
- (a) Weissman, S. I.; Chang, R. *J. Am. Chem. Soc.* **1972**, *94*, 8683-8684. (b) Adriaenssens L. et al. *Chem. Eur. J.* **2009**, *15*, 1072-1076. (c) Liberko, C. A.; Miller, L. L.; Katz, T. J.; Liu, L. *J. Am. Chem. Soc.* **1993**, *115*, 2478-2482. (d) Zak, J. K.; Miyasaka, M.; Rajca, S.; Lapkowski, M.; Rajca, A. *J. Am. Chem. Soc.* **2010**, *132*, 3246-3247. (e) Gilbert, A. M.; Katz, T. J.; Geiger, W. E.; Robben, M. P.; Rheingold, A. L. *J. Am. Chem. Soc.* **1993**, *115*, 3199-3211. (f) Rose-Munch, F.; Li, M.; Rose, E.; Daran, J.-C.; Bossi, A.; Licandro, E.; Mussini, P. R. *Organometallics* **2012**, *31*, 92-104. (g) J. E. Field, T. J. Hill, D. Venkataraman, *J. Org. Chem.* **2003**, *68*, 6071-6078. (g) M. Spassova, I. Asselberghs, T. Verbiest, K. Clays, E. Botek, B. Champagne, *Chem. Phys. Lett.* **2007**, *439*, 213-218.

## Table of Content

